# montalcino, A zebrafish model for variegate porphyria

Dooley, Kimberly A ; Fraenkel, Paula G ; Langer, Nathaniel B ; Schmid, Bettina ; Davidson, Alan J ; Weber, Gerhard ; Chiang, Ken ; Foott, Helen ; Dwyer, Caitlin ; Wingert, Rebecca A ; Zhou, Yi ; Paw, Barry H ; Zon, Leonard I

Abstract: OBJECTIVE Inherited or acquired mutations in the heme biosynthetic pathway leads to a debilitating class of diseases collectively known as porphyrias, with symptoms that can include anemia, cutaneous photosensitivity, and neurovisceral dysfunction. In a genetic screen for hematopoietic mutants, we isolated a zebrafish mutant, montalcino (mno), which displays hypochromic anemia and porphyria. The objective of this study was to identify the defective gene and characterize the phenotype of the zebrafish mutant. MATERIALS AND METHODS Genetic linkage analysis was utilized to identify the region harboring the mno mutation. Candidate gene analysis together with reverse transcriptase polymerase chain reaction was utilized to identify the genetic mutation, which was confirmed via allele-specific oligo hybridizations. Whole mount in situ hybridizations and o-dianisidine staining were used to characterize the phenotype of the mno mutant. mRNA and morpholino microinjections were performed to phenocopy and/or rescue the mutant phenotype. RESULTS Homozygous mno mutant embryos have a defect in the protoporphyrinogen oxidase (ppox) gene, which encodes the enzyme that catalyzes the oxidation of protoporphyrinogen. Homozygous mutant embryos are deficient in hemoglobin, and by 36 hours post-fertilization are visibly anemic and porphyric. The hypochromic anemia of mno embryos was partially rescued by human ppox, providing evidence for the conservation of function between human and zebrafish ppox. CONCLUSION In humans, mutations in ppox result in variegate porphyria. At present, effective treatment for acute attacks requires the administration intravenous hemin and/or glucose. Thus, mno represents a powerful model for investigation, and a tool for future screens aimed at identifying chemical modifiers of variegate porphyria.

DOI: https://doi.org/10.1016/j.exphem.2008.04.008

Published in final edited form as:
*Exp Hematol*. 2008 September ; 36(9): 1132–1142. doi:10.1016/j.exphem.2008.04.008.

# *montalcino*, a Zebrafish Model for Variegate Porphyria

**Kimberly A. Dooley**[1,3], **Paula G. Fraenkel**[1,3], **Nathaniel B. Langer**[2], **Bettina Schmid**[1], **Alan J. Davidson**[1,3], **Gerhard Weber**[1], **Ken Chiang**[1], **Helen Foott**[1], **Caitlin Dwyer**[1], **Rebecca A. Wingert**[1,3], **Yi Zhou**[1], **Barry H. Paw**[2], **Leonard I. Zon**[1], and **Tübingen 2000 Screen Consortium**[†]

1*Division of Hematology/Oncology, Children's Hospital and Dana-Farber Cancer Institute and Harvard Medical School, Howard Hughes Medical Institute, Boston, Massachusetts 02115 USA*

2*Division of Hematology, Brigham & Women's Hospital, Harvard Medical School, Boston, Massachusetts 02115 USA*

## Abstract

**Objective—**Inherited or acquired mutations in the heme biosynthetic pathway lead to a debilitating class of diseases collectively known as porphyrias, with symptoms that can include anemia, cutaneous photosensitivity, and neurovisceral dysfunction. In a genetic screen for hematopoietic mutants, we isolated a zebrafish mutant, *montalcino* (*mno*), which displays hypochromic anemia and porphyria. The objective of this study was to identify the defective gene and characterize the phenotype of the zebrafish mutant.

**Methods—**Genetic linkage analysis was utilized to identify the region harboring the *mno* mutation. Candidate gene analysis together with RT-PCR was utilized to identify the genetic mutation, which was confirmed via allele specific oligo hybridizations. Whole mount in situ hybridizations and 0-dianisidine staining were used to characterize the phenotype of the *mno* mutant. mRNA and morpholino microinjections were performed to phenocopy and/or rescue the mutant phenotype.

**Results—**Homozygous *mno* mutant embryos have a defect in the protoporphyrinogen oxidase (*ppox*) gene, which encodes the enzyme that catalyzes the oxidation of protoporphyrinogen. Homozygous mutant embryos are deficient in hemoglobin, and by 36 hpf are visibly anemic and porphyric. The hypochromic anemia of *mno* embryos was partially rescued by human *ppox*, providing evidence for the conservation of function between human and zebrafish *ppox*.

**Conclusion—**In humans, mutations in *ppox* result in variegate porphyria. At present, effective treatment for acute attacks requires the administration intravenous hemin and/or glucose. Thus, *mno* represents a powerful model for investigation, and a tool for future screens aimed at identifying chemical modifiers of variegate porphyria.

Author for correspondence (e-mail: zon@enders.tch.harvard.edu), HHMI, Children's Hospital of Boston, Boston, MA 02115, Telephone 617-919-2069, Fax 617-730-0222, http://zon.tchlab.org/.

[3]Present addresses: MIT/Broad Institute, Cambridge, Massachusetts 02141 USA (KAD) Massachusetts General Hospital, Boston, Massachusetts USA (AJD; RAW) Division of Hematology/Oncology, Beth Israel Deaconess Medical Center Boston, Massachusetts 02215 (PGF)

[†]Tübingen 2000 Screen Consortium: F. Bebber van, E. Busch-Nentwich, R. Dahm, H. G. Frohnhöfer, H. Geiger, D. Gilmour, S. Holley, J. Hooge, D. Jülich, H. Knaut, F. Maderspacher, C. Neumann, T. Nicolson, C. Nüsslein-Volhard, H. Roehl, U. Schönberger, C. Seiler, C. Söllner, M. Sonawane, A. Wehner, C. Weiler and B. Schmid at the Max-Planck-Institut für Entwicklungsbiologie, Spemannstrasse 35, 72076 Tübingen, Germany. U. Hagner, E. Hennen, C. Kaps, A. Kirchner, T. I. Koblizek, U. Langheinrich, C. Metzger, R. Nordin, M. Pezzuti, K. Schlombs, J. deSantana-Stamm, T. Trowe, G. Vacun, A. Walker and C. Weiler at Artemis Pharmaceuticals/Exelixis Deutchland GmbH, Neurather Ring 1, S51063 Köln, Germany.

### Keywords

ppox; hematopoiesis; porphyria; hypochromia; zebrafish

## Introduction

Porphyrias are a class of diseases resulting from mutations in seven of the eight enzymes in the heme biosynthetic pathway, resulting in an abnormal accumulation of the pathway intermediates, known as porphyrins (reviewed in [1],[2],[3]). The clinical symptoms of the disease can present as an erythrocytic or hepatic syndrome with cutaneous manifestations, depending on the enzyme affected and the site of excess porphyrin accumulation. Variegate porphyria is classified as an acute, hepatic porphyria, and is caused by mutations in *protoporphyrinogen oxidase* (*ppox*). The PPOX enzyme catalyzes the penultimate step of heme biosynthesis, the oxidation of protoporphyrinogen to protoporphyrin in the mitochondria. Clinical symptoms of variegate porphyria can include photocutaneous lesions and neurovisceral dysfunction, including abdominal pain, peripheral neuropathy, and mental disturbances (reviewed in [4]). Treatment of acute attacks primarily involves intravenous hematin administration [2] to inhibit flux through the heme biosynthetic pathway and the associated generation of porphyrins. If untreated, acute attacks can result in long-term or permanent neurological and hepatic damage, or in some cases, can be fatal. While current therapies are effective at treating acute attacks, preventative therapies are needed.

The zebrafish hematopoietic process is conserved throughout vertebrate evolution, as many mouse and human homologues of blood-specific genes have been cloned in zebrafish, including *scl*, *lmo-2*, *gata-1*, and the gene encoding the heme synthetic enzyme *coproporphyrinogen oxidase* (CPO) [5], [6], [7], [8]. Several zebrafish models for hematopoietic disease have been established, including *dracula* and *yquem*, which harbor mutations in the genes encoding the heme biosynthetic enzymes, ferrochelatase and uroporphyrinogen decarboxylase (UROD), respectively [9], [10]. The *dracula* and *yquem* mutants display photosensitive porphyria, with characteristics representative of the corresponding human disease syndromes.

We have characterized the zebrafish porphyric mutant, *mno*, and have cloned the responsible gene, *ppox*. Initially, at the onset of circulation, *mno* displayed normal numbers of red blood cells, but these cells were deficient in hemoglobin. By approximately 36 hpf, there was a visible decrease in circulating erythrocytes, and fluorescence was observed when viewed under epiflourescent light. The *mno* mutant zebrafish could survive to approximately 25 dpf. We further demonstrated that human *ppox* could partially rescue the hypochromia in homozygous mutants, illustrating evolutionary conservation of function. The zebrafish *mno* mutant will be very useful for further elucidating the pathophysiology of variegate porphyria and identifying chemical modifiers of this disease.

## Materials and Methods

### Zebrafish strains and maintenance

Zebrafish were maintained [11] and staged [12] as described previously. $mno^{hq098}$ and $mno^{ia048}$ were identified in the Tübingen 2000 genetic screen, and maintained on the Tü strain. For genetic mapping analyses, outcrosses to the wild-type WIK strain were performed.

### o-dianisidine staining and in-situ hybridization

Detection of hemoglobin by *o*-dianisidine was performed as described [13]. Whole-mount in-situ hybridization with digoxigenin-labeled RNA probes was performed as described [6].

### Meiotic mapping

Homozygous mutant *mno* embryos were collected from pairwise matings of *mno* heterozygotes on the Tu/WIK background. Embryos were scored under a dissection microscope at approximately 48 hours post fertilization (hpf) for anemia. Genomic DNA extraction from individual embryos and bulk segregant analysis were performed as described [14] using primers designed to SSLP markers obtained from the Massachusetts General Hospital Zebrafish Server website (http://zebrafish.mgh.harvard.edu) and synthesized by Invitrogen.

### Isolation of *ppox* cDNA from wild-type and mutant zebrafish

Total RNA was isolated from pools of 20 embryos at 72 hpf using the RNneasy lysis and purification procedure (Qiagen). To obtain cDNA, reverse transcription was performed using Superscript II reverse transcriptase (Invitrogen) in a 20 µl reaction. The reaction was then diluted to 100 µl, and 10 ul of the dilution was used as template for each PCR reaction. The full-length *ppox* cDNA was amplified from both wild type and mutant cDNA using primer PPOX.F (5'-GCGCTGTCCAAATTACATTATTATA-3') and PPOX.R (5'-GCTTCAATCCCAAATAAACAGATGC-3') with the following PCR conditions: 1 cycle of 94°C for 1 min; 39 cycles of 94°C for 1 min, 63°C for 1 min, 72°C for 1 min 30 sec; and 1 cycle of 72°C for 10 min. The RT-PCR products were subcloned into the pCRII vector Plasmid DNA was purified using the Qiagen miniprep kit. Twelve independent clones of wild-type and 10 independent clones of mutant cDNA were sequenced.

### Allele specific oligonucleotide (ASO) hybridization

Individual embryos from a heterozygous cross of *mno*$^{hq098}$ were sorted at 72 hpf according to anemic phenotype and stored in methanol at −20°C. Genomic DNA from the sorted embryos and their PCR amplification were carried out essentially as described [15]. PCR amplifications using genomic DNA as template with the two sets of primers spanning the two respective mutations are as listed: (a) the nonsense mutation (L417X) [F1: 5'-TAAAAACAATCCCTGTAACTCCCAG –3' ; R1: 5'-TAAAAACAATCCCTGTAACTCCCAG –3' ] and (b) the missense mutation (N420S) [F2: 5'- TTATCATCACAGAGGCCATTTATGT -3'; R2: 5'-CTTTAACCACCCACAATTGAAATG -3']. The PCR products were dotted onto nylon membrane using a Schleicher & Schuell manifold and probed with ASO's for the two respective mutations in 3M tetramethyl ammonium chloride (Sigma) as described [16]. The ASO's for the nonsense mutation (L417X) are 5'-ACCTTTAGT**A**AAGCAACGC-3' and 5'-ACCTTTAGT**T**AAGCAACGC-3', respectively for normal and mutant sequences. The ASO's for the missense mutation (N420S) are 5'-TTCTACAGA**A**CTGCATTCC-3' and 5'-TTCTACAGA**G**CTGCATTCC-3', respectively for normal and mutant sequences.

### Morpholino injections

The zebrafish *ppox* intronic sequence was determined by comparison of zebrafish *ppox* cDNA sequence, human genomic *ppox* sequence, and the Sanger Center zebrafish genome sequence database (http://www.sanger.ac.uk/Projects/D_rerio/). Anti-sense morpholino oligos (Gene Tools, Corvalis, Oregon) were designed to target either the ATG start site, or the exon 1/intron boundary sequence (E/I), as follows: PPOX E/I MO (5' – GCT AGT TCT CAC CTC AGA GCC CAG C –3'); PPOX ATG MO (5' – GCT ACA ACC TTC TGC ATT CAG CTC C –3'). Morpholinos were resuspended in Danieau's solution (58 mM NaCl, 0.7 mM KCl, 0.4 mM $MgSO_4$, 0.6 mM $Ca(NO_3)_2$, 5.0 mM Hepes, pH7.6). Wild type or heterozygous mutant

pairwise matings were performed, and the resulting embryos were microinjected between the 1–4 cell stage with 1 nl of morpholino at a final concentration of 0.5 mM. Phenol Red was co-injected as a tracer.

### RNA microinjection

Full length human *ppox* cDNA was obtained from Open Biosystems (GenBank accession #BC002357; vector pOTB7). The full length *ppox* cDNA was subcloned into pCS2+ using EcoRI and XhoI. The resulting clone was linearized with XhoI, and full length mRNA was transcribed from the SP6 promoter using mMessage mMachine according to manufacturer's protocol (Ambion). For rescue experiments, 200 pg or 500 pg of RNA was injected into embryos from pairwise matings of heterozygous *mno* mutants.

### Microarray analysis

Pools of 100 $mno^{hq098-/-}$ and 100 non-sibling wild type embryos were collected at 36 hpf. RNA extraction, target preparation, hybridization, and signal detection were performed as described previously [17].

## Results

The zebrafish mutant, *mno* was identified in a forward genetic, ethylnitrosourea (ENU) mutagenesis screen for embryonic hematopoietic defects. The *mno* mutant was first identified as hypochromic anemic. At 48 hpf, circulating erythrocytes were visualized under a light microscope in $mno^{hq098-/-}$ and wild type sibling embryos. There were fewer cells present in $mno^{hq098-/-}$ embryos than in wild type siblings (data not shown) and the cells in $mno^{hq098-/-}$ embryos lacked the red color indicative of hemoglobinized erythrocytes present in wild type animals (Figure 1A). This phenotype is characteristic of hypochromic anemia in zebrafish [18], [19], [20], [21]. When further observed under epiflourescent illumination using a rhodamine filter, $mno^{hq098-/-}$ embryos exhibited fluorescence in the yolk sac (Figure 1B) and in the tail vessels (Figure 1C), indicative of a porphyric phenotype [9], [10]. The mutation displayed a recessive inheritance pattern, with 25% of embryos from single pairwise matings of heterozygous ($mno^{hq098+/-}$) zebrafish displaying the mutant phenotype.

A second allele, $mno^{ia048}$, was also recovered in the ENU mutagenesis screen. The phenotype of $mno^{ia048-/-}$ embryos is variable, as all homozygous embryos display yolk sac fluorescence, but unlike $mno^{hq098-/-}$, some embryos appear to have hemoglobinized erythrocytes pooling under the yolk sac at 48 hpf under a light microscope (Figure 1D, E). In addition, $mno^{ia048-/-}$ has yolk sac necrosis as early as 48 hpf, which is not observed in $mno^{hq098-/-}$ homozygous mutants. The allelic relationship was confirmed by complementation analysis with $mno^{hq098}$ (data not shown).

Utilizing genetic linkage analysis, the region harboring the *mno* mutation was localized to an approximate 3 cM interval (Figure 1F). Based on local synteny to human chromosome 21, protoporphyrinogen oxidase (*ppox*), the gene encoding the penultimate enzyme in the heme biosynthetic pathway, was identified as a potential candidate for the *mno* mutation. From available partial genomic and cDNA sequences, primers were designed to amplify the entire zf*ppox* coding region from wild type and $mno^{hq098-/-}$ alleles. Subsequent sequencing revealed two single base pair changes in 10 independent pools of $mno^{hq098-/-}$ embryos, T->A at position 1250 and A->G at position 1259. The first mutation, 1250T->A, results in a substitution of a stop codon for leucine at amino acid residue 417 [L417X]. The second mutation results in a substitution of serine for glutamine [N420S], but is presumably non-translated. The identified mutations are shown in Figure 2A.

The two mutations identified in *mno*$^{hq098}$ were confirmed to segregate in a tightly linked Mendelian manner by ASO hybridization (Fig. 2B). Genomic DNA's from individual embryos sorted based on anemic phenotype were amplified by PCR with flanking primers. The amplicons were immobilized onto nylon membranes and hybridized with either normal or mutant sequence ASO's. Oligos corresponding to the 1250T->A and 1259A->G mutations hybridized exclusively to the amplicons from mutant (lanes 5–8) and heterozygous embryos (lanes 1 and 4); oligos corresponding to the normal sequences hybridized exclusively to amplicons from wild type (lanes 2–3) and heterozygous embryos (lanes 1 and 4). The analysis of an additional 48 sorted anemic *mno*$^{hq098-/-}$ embryos showed complete linkage of the two mutant alleles, while 84 sorted, normal embryos were either wild type (n=32) or heterozygous (n=52) genotype (data not shown).

Alignment of the predicted amino acid sequence for zebrafish PPOX with human and mouse proteins reveals a 52% and 50% sequence conservation, respectively (Figure 2C). This sequence is identical to a previous report by [8], except for one amino acid at position 105, which is a leu in our sequence and a pro in the sequence reported by Hanaoka, et al. The corresponding position in mouse and human PPOX is a leu. In human patients, disease associated mutations in the *ppox* gene span the entire protein coding region [22], [23], as indicated by the green and blue arrows in Figure 2C. The region of the protein downstream of the L417X mutation in *mno* (indicated by black arrowhead) contains two conserved residues known to bind the enzymatic cofactor FAD in tobacco protoporphyrinogen oxidase [24], as indicated in Figure 2C.

To confirm that *ppox* is the affected gene in *mno*, we reproduced the mutant phenotype using a morpholino knock-down technique (Figure 3). Wild type embryos were injected at the 1–4 cell stage of development with antisense morpholinos designed to decrease translation or post-transcriptional splicing of *ppox*. Both the number of circulating erythrocytes and fluorescence were evaluated at 48 hpf. In the presence of the morpholino, circulating erythrocytes were not visible (data not shown). Yolk sac fluorescence was observed in 100% (n=88) of injected animals (Figure 3B), in contrast to uninjected wild type embryos (n=104) (Figure 3D). In addition, pericardial edema was observed in morpholino injected animals (Figure 3A, arrows).

To obtain further evidence that the montalcino mutation was due to a defect in *ppox*, embryos from pairwise matings of *mno*$^{hq09+-/-}$ zebrafish were injected at the 1–4 cell stage with an expression construct for human *ppox*. Injected embryos were stained at 36 hpf with o-dianisidine, and genomic DNA was extracted for genotyping. Uninjected siblings served as controls. Of the wild type embryos injected with human *ppox* RNA, normal levels of o-dianisidine staining were observed (Figure 3E). Of the injected homozygous mutant embryos, all 10 embryos displayed partial rescue of hemoglobinized erythrocytes, as indicated by o-dianisidine staining (Figure 3G–H). Consistent with partial rescue of anemia, porphyria was still observed in the hum*ppox* injected mutants (data not shown), suggesting that the endogenous mutant *ppox* is still causing a partial block of heme synthesis and an accumulation of porphyrin.

Expression of zebrafish *ppox* occurs as early as 22 hpf in the intermediate cell mass (ICM), similar to the expression of other hematopoietic genes, including *gata1*, *alas2*, and *β-spectrin* [5], [25], [26]. In *mno* mutants, *ppox* expression in the ICM at 22 hpf is unaltered, as assessed by RNA *in situ* hybridization (Figure 4A). Other early hematopoietic markers were also unaffected, including *scl* and *gata1* (data not shown). We further characterized the onset of the hematopoietic defect by analyzing the temporal expression pattern of erythrocyte specific embryonic *βe3-globin* [27]. At the onset of circulation, approximately 28 hpf, homozygous *mno*$^{hq098-/-}$ embryos display relatively normal numbers of erythrocytes, as shown by *in situ* hybridization for *βe3-globin* (Figure 4B). However, the cells appear deficient in hemoglobin,

as evidenced by pallor of the circulating erythrocytes (data not shown), and the absence of O-dianisidine staining on the ventral yolk sac (Figure 4C). By 48 hpf, *mno*$^{hq098}$ embryos become anemic, confirmed by the absence of expression of *β-globin* (Figure 4D). To assess viability of the mutation, we attempted to raise *mno* homozygotes to adulthood. Only 3/886 survived beyond 7 dpf, and these animals died by approximately 27 dpf. At 25 dpf the surviving mutants appeared stunted, pale, and slightly necrotic (Figure 4E).

To identify genes that display altered regulation, microarray analysis was performed, comparing the expression profiles of wild type and homozygous *mno*$^{hq098}$ embryos at 36 hpf (Table 1). At this time point, there are still circulating erythrocytes in the mutants, but these cells are hypochromic. Many of the downregulated genes in *mno*$^{hq098}$ were erythrocyte specific, including *alas2*, several embryonic *globins* and the membrane structural proteins, *band 4.1* and *band 3*. These results are consistent with the onset of anemia and hypochromia. The number of upregulated genes was much larger, and included a peripheral benzodiazepine receptor and several cytochromes, including *cyt 2b*, *cyt 5*, and *cyt P450*, which utilize heme as part of prosthetic groups. The peripheral-type benzodiazepine receptor has been shown to interact *in vitro* with protoporphyrin IX, the product of the PPOX enzyme, though the *in vivo* function of this interaction is unclear [28], [29], [30].

## Discussion

Utilizing the genetic synteny between human and zebrafish, we have identified a mutation in the *ppox* gene that is responsible for the phenotypic abnormalities of the *mno* mutant. In humans, variegate porphyria is characterized by photosensitivity and neurovisceral dysfunction. The disease is most prevalent in South Africa, where a single C->T transition resulting in an R59W substitution is responsible for the majority of clinical cases [31]. Subsequently, numerous mutations spanning the entire *ppox* gene have been identified in patients with variegate porphyria [22], [23]. The *mno*$^{hq098}$ mutation results in a stop codon in the C-terminal region of the protein, eliminating a region that shares approximately 73% conservation with human PPOX, and contains predicted FAD-binding domains [24].

The majority of human patients with variegate porphyria harbor heteroallelic mutations, and we are aware of only one report of two patients harboring homoallelic mutations [32]. The homoallelic mutations were missense mutations (D349A or A433P) located in the C-terminal region of PPOX, flanking the *mno*$^{hq098}$ mutation. Interestingly, unlike in humans, *mno*$^{hq098+/-}$ heterozygous embryos grow to adulthood with no detectable symptoms of anemia nor porphyria at anytime during development. The *mno*$^{hq098-/-}$ homozygous mutant embryos display autoflourescence and necrosis, but also have anemia. No symptoms of anemia in human variegate porphyria patients have been reported, even in the two patients with the homoallelic mutations [22], [23], [32]. The reasons for these differences are unclear. One possible explanation may be the optical clarity of the developing zebrafish embryo. In zebrafish, the circulating RBCs are exposed to light from the earliest time in development, unlike in humans. This may cause the RBCs to lyse, leading to anemia and ultimate death of the homozygous embryos. The life span of the *mno*$^{hq098-/-}$ embryos is consistent with several other anemic zebrafish mutants, including two alleles of the *chianti* mutant, *cia*$^{hp327}$ and *cia*$^{hs019}$ [21]. Other anemic zebrafish mutants are able to survive to adulthood, for example *sauternes*$^{ty121}$ [25], whereas the porphyric zebrafish mutant *yquem* is embryonic lethal [10]. It is not clear if the ultimate cause of death in the *mno*$^{hq098}$ mutant zebrafish embryos is due to the anemia and/or a toxic accumulation of porphyrins.

Partial rescue of the *mno*$^{hq098-/-}$ phenotype by overexpression of human *ppox* demonstrates the functional conservation of the enzyme across species. However, despite the partial rescue of hemoglobinized erythrocytes, the autoflourescent phenotype was still observed. Given that

in human patients, the disease has an autosomal dominant inheritance pattern, the endogenous homozygous mutant PPOX in the partially rescued zebrafish may still be diverting flux of the heme biosynthetic pathway, resulting in an accumulation of toxic porphyrins.

Using microarray analysis, many genes were identified as aberrantly regulated in the *mno* mutant. Most of the downregulated genes were erythrocyte specific, such as several embryonic beta globins and *band3* [33], correlating with the decrease in circulating red blood cells observed at 36 hpf. A much larger number of genes were shown to be upregulated, including several cytochromes and a benzodiazepine receptor. The cytochromes utilize heme in the prosthetic groups, and the upregulation may reflect a positive feedback loop when heme is limiting. The peripheral-type benzodiazepine receptor (PBR) is associated with numerous biological functions, including porphyrin transport and neurological and neuropsychiatric diseases (reviewed in [34]). PBR has been shown to bind protoporphyrin IX, the product of PPOX, with nanomolar affinity *in vitro*. However, the endogenous function of this interaction has not been defined (reviewed in [35]). The underlying basis of the neurological symptoms of porphyria is not well understood. Future investigations into the relationship between PBR and porphyrins may lead to treatments for the neurological aspects of variegate porphyria, as well as other classes of porphyria.

The list of upregulated genes observed in *mno* mutants also included apolipoproteins, corticosteroids, and very long chain acyl coA synthetase, genes important for steroid biosynthesis and fatty acid metabolism. A report [36] has revealed a previously unknown link between the liver specific 5-aminolevulinate synthase 1 (ALAS1) and peroxisome proliferator-activated receptor γ coactivator 1α (PGC-1α), a transcriptional coactivator whose expression is upregulated during fasting. Unlike ALAS2, ALAS1 is ubiquitously expressed, and its primary role in the liver is the generation of heme for cytochrome biosynthesis. Several dietary factors, including fasting, are known to precipitate acute porphyric attacks by an unknown mechanism. Handschin and colleagues demonstrate that PGC-1α mediates an increase in ALAS1 expression during fasting, increasing the level of heme precursors, which precipitates acute porphyric attacks in patients with defects in heme biosynthetic enzymes. Here, steroid and fatty acid genes upregulated in the microarray analysis represent another link between the nutritional status and porphyria. Future investigation will elucidate the significance of this relationship.

Several other zebrafish mutants display a porphyric phenotype, including *yquem* [10], *dracula* [9], and *freixenet* [13]. In *yquem* and *dracula* mutants, the affected heme biosynthetic enzymes are ferrochetalase and UROD, respectively. More recently, a zebrafish model for coproporphyria (HCP) was created by injecting a morpholino targeting coproporphyrinogen oxidase (CPO) [8]. In addition, the previously identified zebrafish mutants, *shiraz* [37] and *sauternes* [25] both have hypochromic anemia, but are not porphyric. The *shiraz* mutation is within the *glutaredoxin* 5 gene, which has a downstream effect on ALAS2 activity, whereas the *sauternes* mutation is in the *alas2* gene itself. Thus, as in humans, ALAS2 mutations do not result in porphyria. The heme biosynthetic pathway is highly conserved between zebrafish and humans, and the *mno* mutant therefore represents a powerful model to dissect the underlying mechanisms of variegate porphyria and a means to identify potential new therapies.

## Acknowledgments

KAD was supported by a fellowship from the American Cancer Society and the NIH. BHP and LIZ were supported by the NIH. LIZ is an investigator of the HHMI.

## References


1. Sassa S. The Porphyrias. Photodermatol Photoimmunol Photomed 2002;18:56–67. [PubMed: 12147038]
2. Sassa S. Hematological Aspects of the Porphyrias. Int J Hematol 2000;71:1–17. [PubMed: 10729988]
3. Chemmanur AT, Bonkovsky HL. Hepatic porphyrias: diagnosis and management. 2004;8(4):807–838.
4. Anderson KE, Bloomer JR, Bonkovsky HL, et al. Recommendations for the diagnosis and treatment of the acute porphyrias. Ann Intern Med 2005;142(6):439–450. [PubMed: 15767622]
5. Detrich HW 3rd, Kieran MW, Chan FY, et al. Intraembryonic hematopoietic cell migration during vertebrate development. Proc Natl Acad Sci U S A 1995;92(23):10713–10717. [PubMed: 7479870]
6. Thompson MA, Ransom DG, Pratt SJ, et al. The cloche and spadetail genes differentially affect hematopoiesis and vasculogenesis. Dev Biol 1998;197(2):248–269. [PubMed: 9630750]
7. Liao EC, Paw BH, Oates AC, Pratt SJ, Postlethwait JH, Zon LI. SCL/Tal-1 transcription factor acts downstream of cloche to specify hematopoietic and vascular progenitors in zebrafish. Genes Dev 1998;12(5):621–626. [PubMed: 9499398]
8. Hanaoka R, Katayama S, Dawid IB, Kawahara A. Characterization of the heme synthesis enzyme coproporphyrinogen oxidase (CPO) in zebrafish erythrogenesis. Genes Cells 2006;11(3):293–303. [PubMed: 16483317]
9. Childs S, Weinstein BM, Mohideen MA, Donohue S, Bonkovsky H, Fishman MC. Zebrafish dracula encodes ferrochelatase and its mutation provides a model for erythropoietic protoporphyria. Curr Biol 2000;10(16):1001–1004. [PubMed: 10985389]
10. Wang H, Long Q, Marty SD, Sassa S, Lin S. A zebrafish model for hepatoerythropoietic porphyria. Nat Genet 1998;20(3):239–243. [PubMed: 9806541]
11. Westerfield, M. The Zebrafish Book. University of Oregon Press; 1993.
12. Kimmel CB, Ballard WW, Kimmel SR, Ullmann B, Schilling TF. Stages of embryonic development of the zebrafish. Dev Dyn 1995;203(3):253–310. [PubMed: 8589427]
13. Ransom DG, Haffter P, Odenthal J, et al. Characterization of zebrafish mutants with defects in embryonic hematopoiesis. Development 1996;123:311–319. [PubMed: 9007251]
14. Zhang J, Talbot WS, Schier AF. Positional cloning identifies zebrafish one-eyed pinhead as a permissive EGF-related ligand required during gastrulation. Cell 1998;92(2):241–251. [PubMed: 9458048]
15. Johnson SL, Midson CN, Ballinger EW, Postlethwait JH. Identification of RAPD primers that reveal extensive polymorphisms between laboratory strains of zebrafish. Genomics 1994;19(1):152–156. [PubMed: 8188217]
16. Farr CJ, Saiki RK, Erlich HA, McCormick F, Marshall CJ. Analysis of RAS gene mutations in acute myeloid leukemia by polymerase chain reaction and oligonucleotide probes. Proc Natl Acad Sci U S A 1988;85(5):1629–1633. [PubMed: 3278322]
17. Weber GJ, Choe SE, Dooley KA, Paffett-Lugassy NN, Zhou Y, Zon LI. Mutant-specific gene programs in the zebrafish. Blood 2005;106(2):521–530. [PubMed: 15827125]
18. Donovan A, Brownlie A, Dorschner MO, et al. The zebrafish mutant gene chardonnay (cdy) encodes divalent metal transporter 1 (DMT1). Blood 2002;100(13):4655–4659. [PubMed: 12393445]
19. Donovan A, Brownlie A, Zhou Y, et al. Positional cloning of zebrafish ferroportin1 identifies a conserved vertebrate iron exporter. Nature 2000;403(6771):776–781. [PubMed: 10693807]
20. Wingert RA, Galloway JL, Barut B, et al. Deficiency of glutaredoxin 5 reveals Fe-S clusters are required for vertebrate haem synthesis. Nature 2005;436(7053):1035–1039. [PubMed: 16110529]
21. Wingert RA, Brownlie A, Galloway JL, et al. The chianti zebrafish mutant provides a model for erythroid-specific disruption of transferrin receptor 1. Development 2004;131(24):6225–6235. [PubMed: 15563524]
22. Wiman A, Harper P, Floderus Y. Nine novel mutations in the protoporphyrinogen oxidase gene in Swedish families with variegate porphyria. Clin Genet 2003;64(2):122–130. [PubMed: 12859407]
23. von und zu Fraunberg M, Timonen K, Mustajoki P, Kauppinen R. Clinical and biochemical characteristics and genotype-phenotype correlation in Finnish variegate porphyria patients. Eur J Hum Genet 2002;10(10):649–657. [PubMed: 12357337]

24. Koch M, Breithaupt C, Kiefersauer R, Freigang J, Huber R, Messerschmidt A. Crystal structure of protoporphyrinogen IX oxidase: a key enzyme in haem and chlorphyll biosynthesis. EMBO Journal 2004;23(8):1720–1728. [PubMed: 15057273]
25. Brownlie A, Donovan A, Pratt SJ, et al. Positional cloning of the zebrafish sauternes gene: a model for congenital sideroblastic anaemia. Nat Genet 1998;20(3):244–250. [PubMed: 9806542]
26. Liao EC, Paw BH, Peters LL, et al. Hereditary spherocytosis in zebrafish riesling illustrates evolution of erythroid beta-spectrin structure, and function in red cell morphogenesis and membrane stability. Development 2000;127(23):5123–5132. [PubMed: 11060238]
27. Brownlie A, Hersey C, Oates AC, et al. Characterization of embryonic globin genes of the zebrafish. Dev Biol 2003;255(1):48–61. [PubMed: 12618133]
28. Verma A, Nye JS, Snyder SH. Porphyrins are endogenous ligands for the mitochondrial (peripheral-type) benzodiazepine receptor. Proc Natl Acad Sci U S A 1987;84(8):2256–2260. [PubMed: 3031675]
29. Cantoni L, Rizzardini M, Skorupska M, et al. Hepatic protoporphyria is associated with a decrease in ligand binding for the mitochondrial benzodiazepine receptors in the liver. Biochem Pharmacol 1992;44(6):1159–1164. [PubMed: 1329761]
30. Wendler G, Lindemann P, Lacapere JJ, Papadopoulos V. Protoporphyrin IX binding and transport by recombinant mouse PBR. Biochem Biophys Res Commun 2003;311(4):847–852. [PubMed: 14623258]
31. Meissner PN, Dailey TA, Hift RJ, et al. A R59W mutation in human protoporphyrinogen oxidase results in decreased enzyme activity and is prevalent in South Africans with variegate porphyria. Nat Genet 1996;13(1):95–97. [PubMed: 8673113]
32. Roberts AG, Puy H, Dailey TA, et al. Molecular characterization of homozygous variegate porphyria. Hum Mol Genet 1998;7(11):1921–1925. [PubMed: 9811936]
33. Paw BH, Davidson AJ, Zhou Y, et al. Cell-specific mitotic defect and dyserythropoiesis associated with erythroid band 3 deficiency. Nat Genet 2003;34(1):59–64. [PubMed: 12669066]
34. Papadopoulos V. In search of the function of the peripheral-type benzodiazepine receptor. Endocr Res 2004;30(4):677–684. [PubMed: 15666811]
35. Gavish M, Bachman I, Shoukrun R, et al. Enigma of the peripheral benzodiazepine receptor. Pharmacol Rev 1999;51(4):629–650. [PubMed: 10581326]
36. Handschin C, Lin J, Rhee J, et al. Nutritional regulation of hepatic heme biosynthesis and porphyria through PGC-1alpha. Cell 2005;122(4):505–515. [PubMed: 16122419]
37. Wingert RA, Galloway JL, Barut B, et al. Deficiency of glutaredoxin 5 reveals Fe-S clusters are required for vertebrate haem synthesis. Nature 2005;436(7053):1035–1039. [PubMed: 16110529]

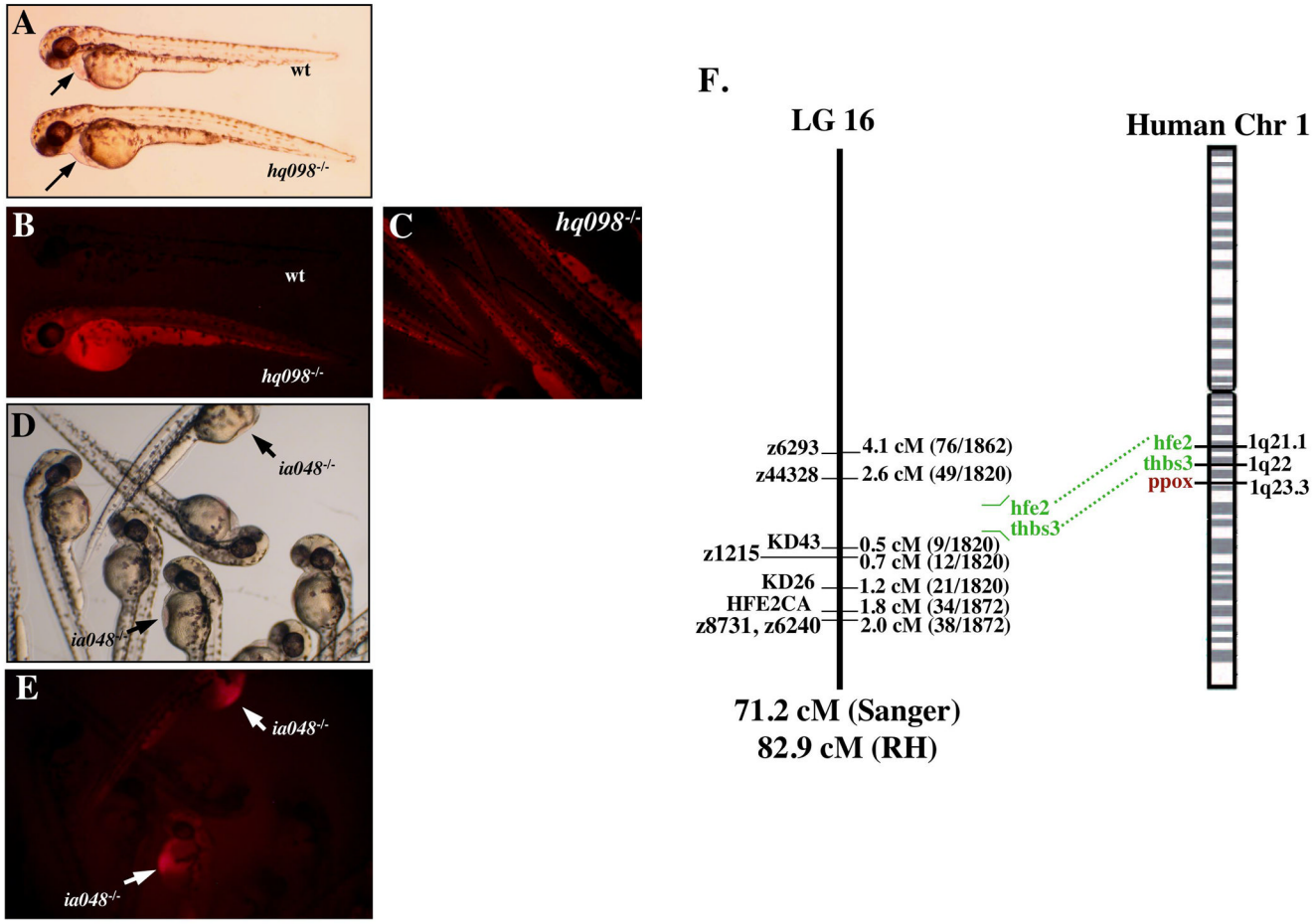


**Figure 1. Blood phenotype and genetic linkage analysis of *montalcino***

Homozygous mutant embryos (*mno*$^{hq098-/-}$) display hypochromic anemia at 48 hpf under bright light. A) Arrows indicate the cardiac region, where red tint of red blood cells (RBC) can be seen in the wild type animals but not homozygous mutant siblings. B) In contrast to wild type siblings (top), *mno*$^{hq098-/-}$ embryos (bottom) display autoflourescence when analyzed under a flourescent light microscope with a Texas Red filter. C) Autoflourescence can be visualized in the posterior tail vessels of *mno*$^{hq098-/-}$ embryos. D) At 48 hpf, homozygous mutant embryos (*mno*$^{ia048-/-}$) under display pooling of RBCs under the yolk sac (arrows). E) When viewed under a fluorescent light microscope with a Texas Red filter, these same *mno*$^{ia048-/-}$ embryos display autoflourescence in the yolk sacs, in contrast to wild type siblings (no arrows). F) Genetic linkage analysis localized the mutation to LG16. Syntenic relationship between human chromosome 1 and zebrafish LG 16 identified the *ppox* gene as a candidate for the genetic lesion.

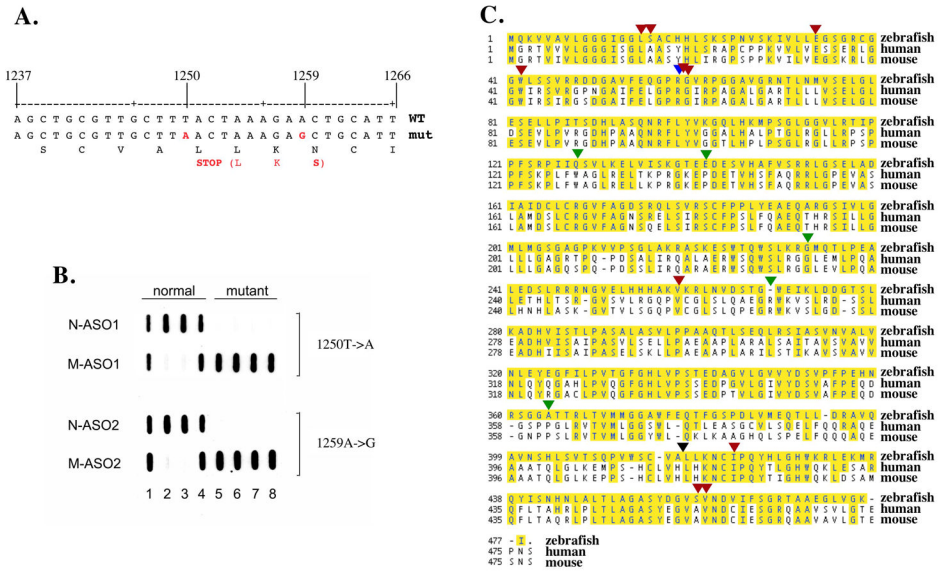


**Figure 2. Mutation in *ppox* of *mno*$^{hq098-/-}$ results in premature stop codon**

A) RT-PCR was performed on pools of homozygous wt or homozygous mutant embryos. The entire *ppox* cDNA was sequenced, revealing single base pair changes as indicated. The first T ->A mutation at position 1250 results in premature translational termination, and the second, presumably non-translated, A->G mutation, results in serine for glutamine substitution. B) Genomic DNA from individual embryos, sorted based on anemic phenotype, was amplified using primers flanking the mutated region identified from the cDNA sequencing. Allele specific oligo hybridization confirmed the presence of both single base pair mutations in mutant embryos, as shown. An additional 48 homozygous mutants, 52 heterozygous wild type, and 32 homozygous wild type embryos further confirmed linkage (not shown). C) Alignment of zebrafish ppox with human and mouse. (black arrow - position of stop generated in *mno*$^{hq098-/-}$ ; blue arrow - south African mutation, R59W; green arrow - mutations identified in human patients; red arrow - FAD binding residues, human).

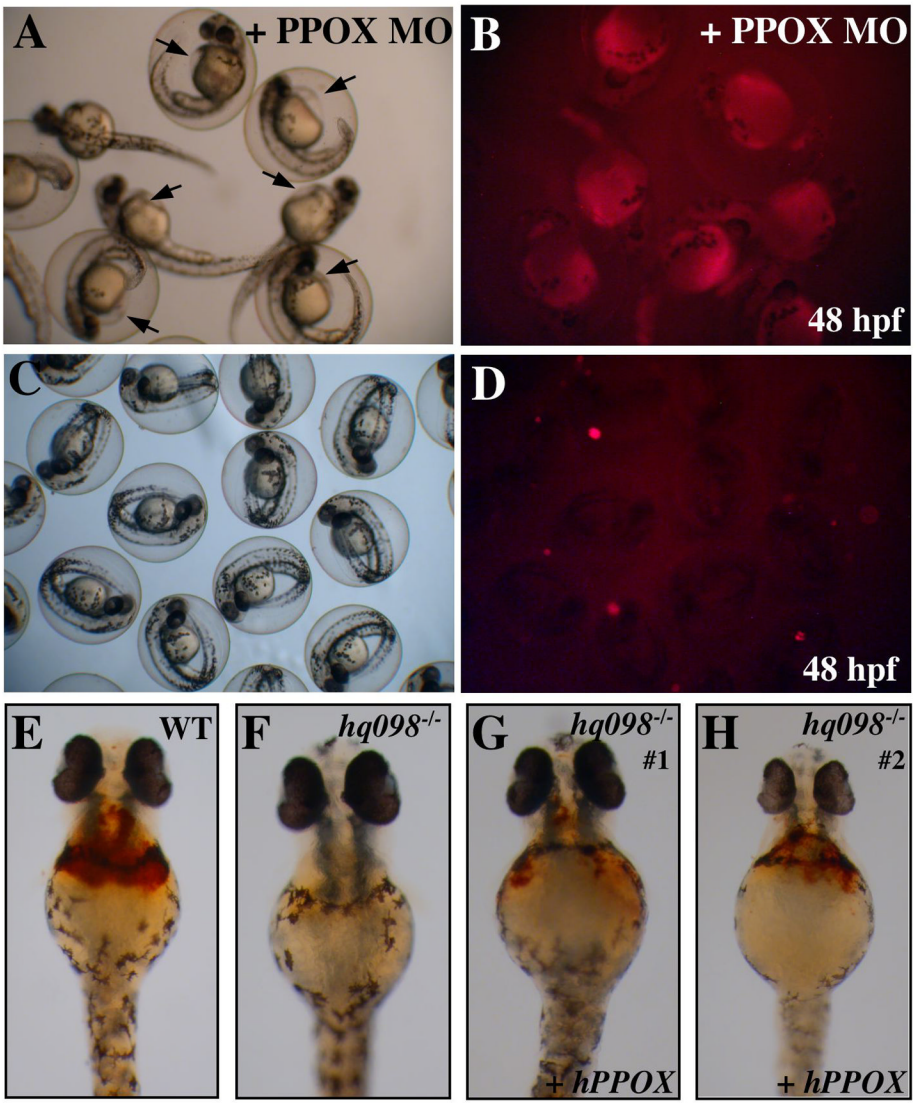


**Figure 3. Morpholino knockdown and RNA rescue confirm *ppox* as the gene responsible for defects in *montalcino***

Wild type embryos were injected with ppox MO and assayed for fluorescence. A,B) Live images of injected wild type embryos at 48 hpf under bright light (A) or bright light with a Texas Red Filter (B). Injected embryos display pericardial edemia (arrows in (A)) and fluorescence in RBC and yolk sac (B). C,D) Control, uninjected wild type embryos at 48 hpf. E–H) Embryos from pairwise mating of $mno^{hq098+/-}$ were injected with full length, human *ppox* RNA and stained with o-dianisidine at 48 hpf, to detect hemoglobinized RBC. E) Wild type uninjected embryo. F) uninjected $mno^{hq098-/-}$ , G, H) Injected $mno^{hq098-/-}$.

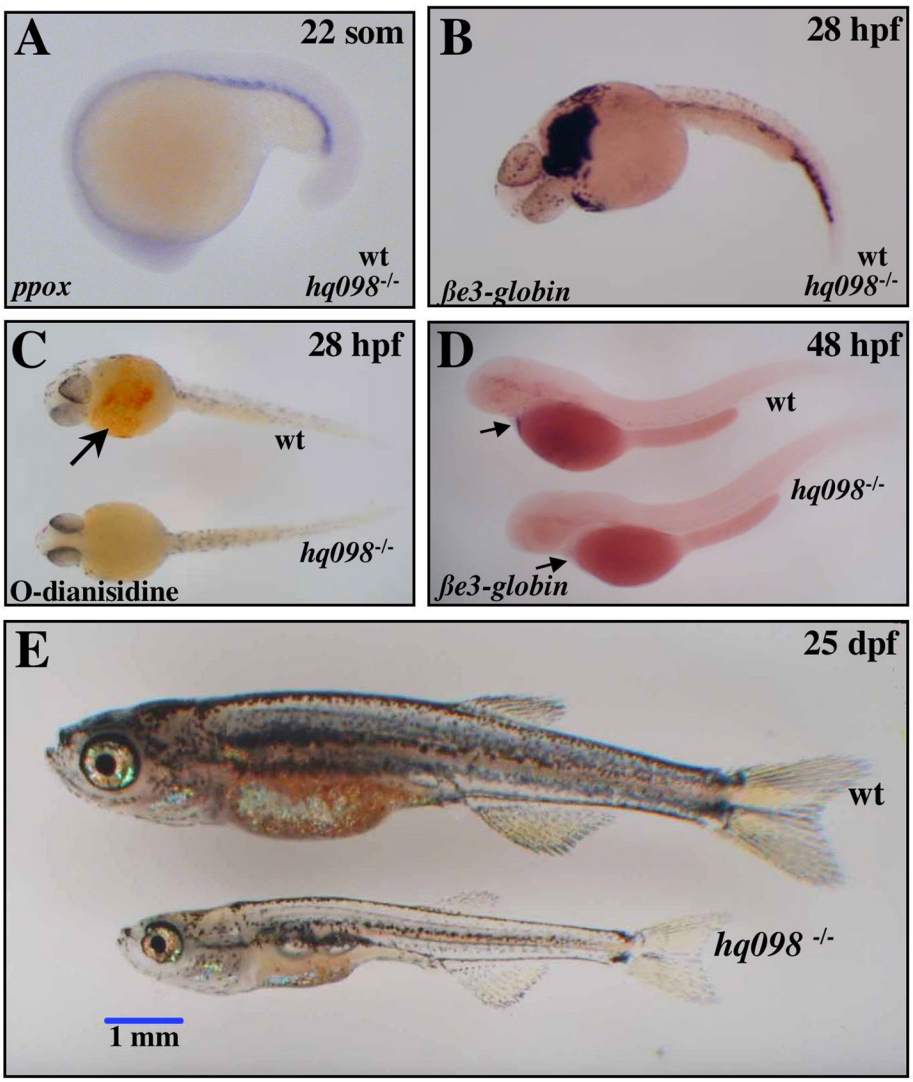


**Figure 4. Hematopoietic phenotype of *montalcino***

A) RNA *in situ* hybridizations were performed on embryos from pairwise matings of *mno*$^{hq098+/-}$. A) zf*ppox* was expressed to wild type levels in the ICM of 100% of animals. B) At 28 hpf, *βe3-globin* was expressed to wild type levels in circulating RBC of 100% of animals, indicating normal numbers of circulating erythrocytes in *mno*$^{hq098-/-}$ embryos. C) o-dianisidine staining for hemoglobinized erythrocytes at 28 hpf revealed early onset hypochromia in 25% of animals. D) at 48 hpf, loss of *βe3-globin* expression in 25% of animals revealed anemia. E) The phenotype at 25 dpf of the very few animals that survive past day 7 is shown. Animals are pale, short, and have regions of necrosis. None were able to survive past day 28.

## Table 1

### Microarray analysis of *montalcino* embryos at 36 hpf

| UniGene Annotation | Probe Set ID | Mean Fold Change (log based) |
|---|---|---|
| Cleavage and polyadenylation specificity factor, 73 kDa subunit | Dr.24764.1.S1_at | 2.59 |
| Forkhead box protein L1 (Forkhead-related protein FKHL11) (Transcription factor FKH | Dr.15390.1.A1_at | 2.47 |
| embryonic globin beta e2 | DrAffx.2.15.S1_at | 2.42 |
| zona pellucida glycoprotein 4 preproprotein | Dr.19916.2.A1_s_at | 2.23 |
| alas2: aminolevulinate, delta-, synthetase 2 | Dr.8180.1.S1_at | 1.58 |
| Danio rerio erythroid band 3 anion exchanger 1 (ae1) | Dr.20971.1.S2_at | 1.47 |
| D-amino acid oxidase | Dr.3663.1.A1_at | 1.46 |
| epb41: erythrocyte membrane protein band 4.1 (elliptocytosis 1, RH-linked) | Dr.3027.1.S1_at | 1.41 |
| | Dr.6952.1.A1_at | 1.30 |
| MAP kinase-interacting serinethreonine kinase 1; MAP kinase interacting kinase 1 | Dr.25422.1.S1_s_at | 1.10 |
| hbae3: hemoglobin alpha embryonic-3 | Dr.1450.1.S1_s_at | 1.10 |
| JC2436 5-nucleotidase | Dr.3959.1.A1_at | 0.99 |
| pklr: pyruvate kinase, liver and RBC | Dr.1699.1.A1_at | 0.95 |
| hbae3: hemoglobin alpha embryonic-3 | Dr.1450.1.S1_at | 0.90 |
| Embryonic Globin gene Be1 | DrAffx.1.85.S1_s_at | 0.66 |
| rbp4: retinol binding protein 4, plasma | Dr.5479.1.S1_at | −0.55 |
| hspa9b: heat shock protein 9B | Dr.4503.1.S2_at | −0.64 |
| keratin 21, type I, cytoskeletal - rat | Dr.12425.2.S1_a_at | −0.66 |
| hspd1: heat shock 60kD protein 1 (chaperonin) | Dr.7108.1.S1_at | −0.67 |
| NADH dehydrogenase | Dr.434.1.S1_at | −0.67 |
| DnaJ (Hsp40) homolog, subfamily A, member 2 | Dr.25140.2.S1_at | −0.73 |
| | Dr.19902.3.S1_at | −0.74 |
| Keratin, type I cytoskeletal 14 | Dr.12425.5.S1_a_at | −0.77 |
| CGI-107 protein [Homo sapiens | Dr.24930.1.S1_at | −0.78 |
| succinate dehydrogenase complex, subunit A, flavoprotein (Fp) | Dr.11239.1.S1_at | −0.78 |
| ucp2: uncoupling protein 2 | Dr.21244.1.S1_at | −0.79 |
| | Dr.2518.1.A1_at | −0.80 |
| sod1: superoxide dismutase 1, soluble | Dr.20938.1.S1_at | −0.81 |
| RDH1_HUMAN 11-cis retinol dehydrogenase | Dr.13301.1.S1_at | −0.83 |
| | Dr.11029.1.A1_at | −0.86 |
| hspa9b: heat shock protein 9B | Dr.4503.1.S1_at | −0.87 |
| Cystathionine gamma-lyase | Dr.3560.1.A1_at | −0.93 |
| mat2a: methionine adenosyltransferase II, alpha | Dr.2850.1.S1_at | −0.96 |
| probable flavoprotein-ubiquinone oxidoreductase | Dr.24219.5.S1_at | −0.96 |
| anti-sigma cross-reacting protein homolog I alpha precursor - human | Dr.6709.1.S1_at | −0.98 |
| | Dr.467.1.A1_at | −0.99 |
| Kelch-like ECH-associated protein 1 (Cytosolic inhibitor of Nrf2) | Dr.6806.1.S1_at | −1.03 |
| Apolipoprotein D precursor (Apo-D) (ApoD). | Dr.15815.1.A1_at | −1.03 |
| HIV gp120-binding C-type lectin - human | Dr.14963.1.A1_at | −1.04 |
| Cytochrome c-type heme lyase | Dr.4423.1.S1_at | −1.06 |
| similar to photorepair | Dr.23983.1.A1_at | −1.07 |
| helicase, lymphoid specific; proliferation-associated SNF2-like [Mus musculus] | Dr.26546.1.A1_at | −1.10 |
| | Dr.19.1.A1_at | −1.10 |
| Heat shock protein 67B2 | Dr.18607.1.S1_at | −1.11 |
| COX15 homolog, isoform 1 precursor; cytochrome c oxidase subunit 15; cytochrome c | Dr.11635.1.A1_at | −1.11 |
| gclc: glutamate-cysteine ligase, catalytic subunit | Dr.7271.1.S1_at | −1.14 |
| CYR61 protein precursor (Cysteine-rich, angiogenic inducer, 61)(Insulin-like growth fac | Dr.15501.1.S1_at | −1.14 |
| hig1: hypoxia induced gene 1 | Dr.13321.1.S2_at | −1.15 |
| Tubulin beta-2 chain | Dr.23801.1.A1_at | −1.17 |
| | Dr.14702.1.A1_at | −1.19 |
| SURF-1 protein - mouse | Dr.14568.1.S1_at | −1.19 |
| benzodiazepine receptor, peripheral-type - human | Dr.20778.1.S1_at | −1.20 |
| probable thioredoxin peroxidase | Dr.10624.1.S1_at | −1.20 |
| hypothetical protein FLJ20487 [Homo sapiens]. | Dr.8010.1.S1_at | −1.22 |
| | Dr.3266.1.A1_at | −1.23 |
| | Dr.22988.1.A1_at | −1.23 |
| hypothetical protein PP591 | Dr.13364.1.S1_at | −1.24 |
| core1 UDP-galactose:N-acetylgalactosamine-alpha-R beta 1,3-galac | Dr.6223.1.A1_at | −1.25 |
| Corticosteroid 11-beta-dehydrogenase, isozyme 1 | Dr.16029.1.S1_at | −1.27 |
| | Dr.1870.1.A1_at | −1.27 |
| Retinoic acid-binding protein II, cellular | Dr.25576.1.A1_at | −1.29 |
| RAD51-like 1 isoform 1 | Dr.17199.1.S1_at | −1.29 |
| titin, cardiac muscle | Dr.11748.1.A1_at | −1.29 |
| alpha-A crystallin | Dr.17476.1.A1_at | −1.30 |
| retinol dehydrogenase 14 (all-trans and 9-cis); PAN2 protein | Dr.21921.1.A1_at | −1.32 |
| hig1: hypoxia induced gene 1 | Dr.13321.1.S1_at | −1.33 |

| UniGene Annotation | Probe Set ID | Mean Fold Change (log based) |
|---|---|---|
| epoxide hydrolase | Dr.17186.1.S1_at | −1.33 |
| probable thioredoxin peroxidase | Dr.10624.2.S1_at | −1.39 |
| dio1: deiodinase, iodothyronine, type I | Dr.24960.1.S1_at | −1.41 |
| Selenoprotein X 1 | Dr.13967.1.A1_at | −1.43 |
| | Dr.21377.1.A1_at | −1.43 |
| | Dr.3429.1.A1_at | −1.46 |
| helicase, lymphoid specific; proliferation-association SNF2-like [Mus musculus] | Dr.4544.1.S1_at | −1.46 |
| IRG1_MOUSE IMMUNE-RESPONSIVE PROTEIN 1 | Dr.10914.1.A1_at | −1.47 |
| | Dr.5517.1.A1_at | −1.50 |
| probable thioredoxin peroxidase | Dr.10624.2.S1_a_at | −1.57 |
| | Dr.5517.2.S1_at | −1.63 |
| Very-long-chain acyl-CoA synthetase | Dr.12740.1.A1_at | −1.63 |
| | Dr.26514.1.A1_at | −1.66 |
| tef: thyrotroph embryonic factor | Dr.578.1.A1_at | −1.73 |
| NADPH-cytochrome P450 reductase | Dr.13867.1.A1_at | −1.80 |
| cry2b: cryptochrome 2b | Dr.10330.1.S1_at | −1.81 |
| tef: thyrotroph embryonic factor | Dr.578.2.S1_a_at | −1.83 |
| lipocalin-type prostaglandin D synthase-like protein | Dr.1192.1.S1_at | −1.85 |
| | Dr.18661.1.A1_at | −1.86 |
| 55 KDA ERYTHROCYTE MEMBRANE PROTEIN | Dr.17659.1.S1_at | −1.90 |
| | Dr.6401.1.S1_at | −2.00 |
| xeroderma pigmentosum group C repair complementing protein p12 | Dr.4069.1.A1_at | −2.16 |
| Proline oxidase, mitochondrial precursor | Dr.12460.1.A1_at | −2.23 |
| cry5: cryptochrome 5 | Dr.10332.1.S1_at | −2.25 |
| abhydrolase domain containing 4 [Homo sapiens]. | Dr.14922.1.A1_at | −2.29 |
| xeroderma pigmentosum group C repair complementing protein p125 | Dr.19728.1.A1_at | −2.30 |
| lipocalin-type prostaglandin D synthase-like protein | Dr.1192.1.S1_a_at | −2.32 |
| period 2 circadian clock protein | DrAffx.2.2.S1_at | −2.33 |
| cytochrome P450, subfamily IIJ | Dr.11609.1.S1_at | −2.36 |
| | Dr.16830.1.A1_at | −2.37 |
| | Dr.18657.1.S1_at | −2.40 |
| | Dr.12142.1.A1_at | −2.42 |
| | Dr.23516.1.S1_at | −2.43 |
| mpx: myeloid-specific peroxidase | Dr.9478.2.S1_at | −2.47 |
| per2: period homolog 2 (Drosophila) | Dr.6754.1.A1_at | −2.48 |
| 92 kDa type IV collagenase precursor (MMP-9) | Dr.967.1.S1_at | −2.51 |
| | Dr.12694.1.A1_at | −2.52 |
| ribonucleoside-diphosphate reductase | Dr.2906.1.S1_at | −2.53 |
| | Dr.23441.1.S1_at | −2.68 |
| weakly similar to Estradiol 17 beta-dehydrogenase 4 | Dr.8914.1.S1_at | −2.71 |
| mpx: myeloid-specific peroxidase | Dr.9478.1.S1_at | −2.77 |
| heme binding protein 2 | Dr.18410.1.S1_at | −2.80 |
| zcry-dash: cryptochrome dash | Dr.18310.2.A1_at | −2.86 |
| | Dr.18657.2.A1_at | −2.88 |
| | Dr.9849.1.A1_at | −2.90 |
| zcry-dash: cryptochrome dash | Dr.18310.1.S1_at | −2.97 |
| vg1: vitellogenin 1 | Dr.25009.6.A1_a_at | −2.99 |
| | Dr.21447.1.A1_at | −3.02 |
| Heat shock cognate 71 kDa protein | Dr.25639.1.A1_at | −3.02 |
| | Dr.23741.1.S1_at | −3.09 |
| ATP-binding cassette, sub-family G, member 2; breast cancer resistance protein; mito | Dr.22153.1.A1_at | −3.17 |
| | Dr.7799.1.A1_at | −3.22 |
| nuclear factor, interleukin 3, regulated [Rattus norvegicus] | Dr.17447.1.A1_at | −3.24 |
| lipocalin-type prostaglandin D synthase-like protein, | Dr.1192.2.S1_at | −3.67 |
| apolipoprotein D - mouse | Dr.16052.1.S1_at | −3.69 |
| Complement component C7 precursor | Dr.96.1.A1_at | −3.70 |
| cartilage acidic protein 1 | Dr.6210.1.S1_at | −3.82 |
| fos: v-fos FBJ murine osteosarcoma viral oncogene homolog | Dr.12986.2.S1_at | −3.93 |
| | Dr.17061.1.A1_at | −4.88 |